Supplement of Atmos. Chem. Phys., 21, 3593–3605, 2021
https://doi.org/10.5194/acp-21-3593-2021-supplement

Atmospheric Chemistry and Physics
Open Access
EGU

Supplement of

Sensitivity of modeled Indian monsoon to Chinese and Indian aerosol emissions

Peter Sherman et al.

Correspondence to: Michael B. McElroy (mbm@seas.harvard.edu)

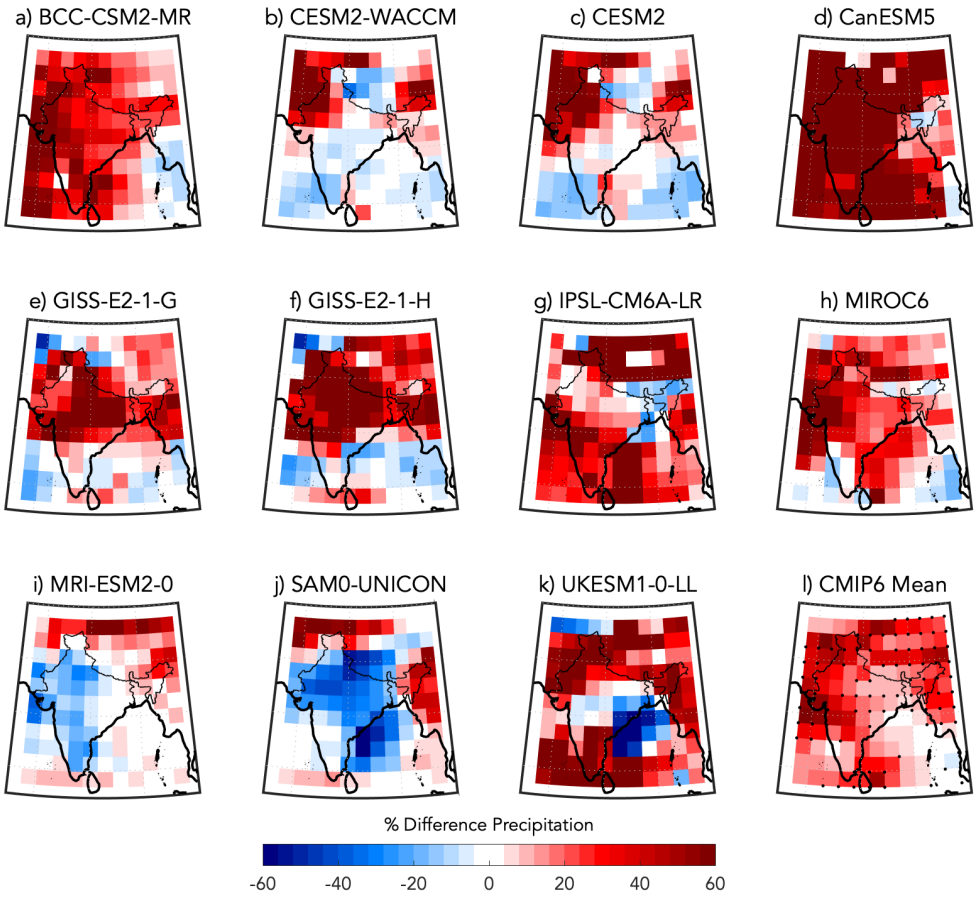

Figure S1. (a-k) CMIP6 JJAS percent difference in precipitation after three decades of simulation between a quadrupling of preindustrial CO_2 concentrations (4xCO2) and preindustrial control (piControl) runs. (l) CMIP6 ensemble mean percent difference between 4xCO2 and piControl. Stippled grid cells denote regions where 70% of the models agree on the sign of the change.

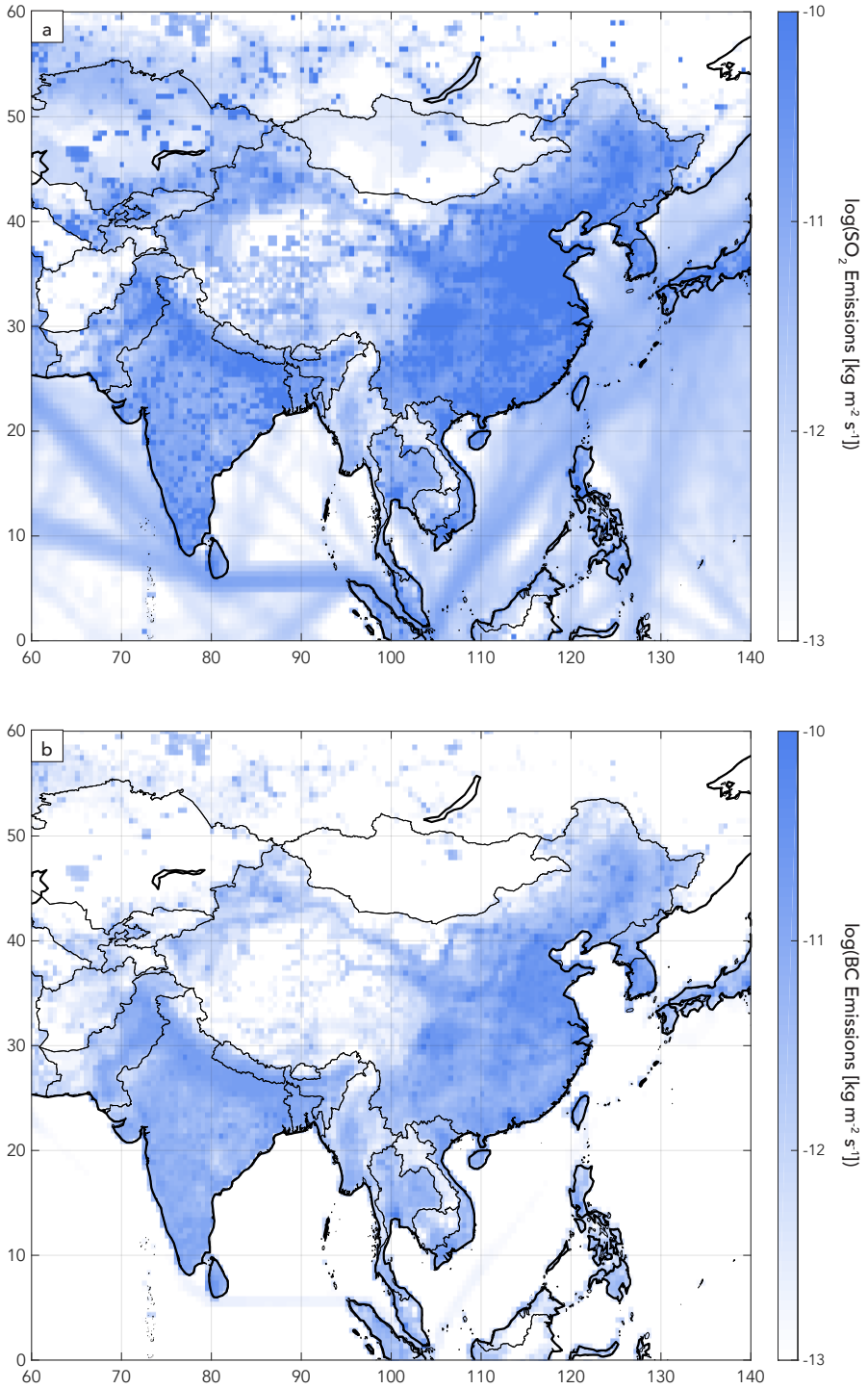

Figure S2. The mean monthly source of anthropogenic emissions [kg m^{-2} s^{-1}] of (a) SO_2 and (b) BC in South and East Asia used as the control input for the PDRMIP and RAEI experiments averaged over the period 2000 to 2015. Note the logarithmic color bar axis in both figures. Emissions data are from Hoesly et al.

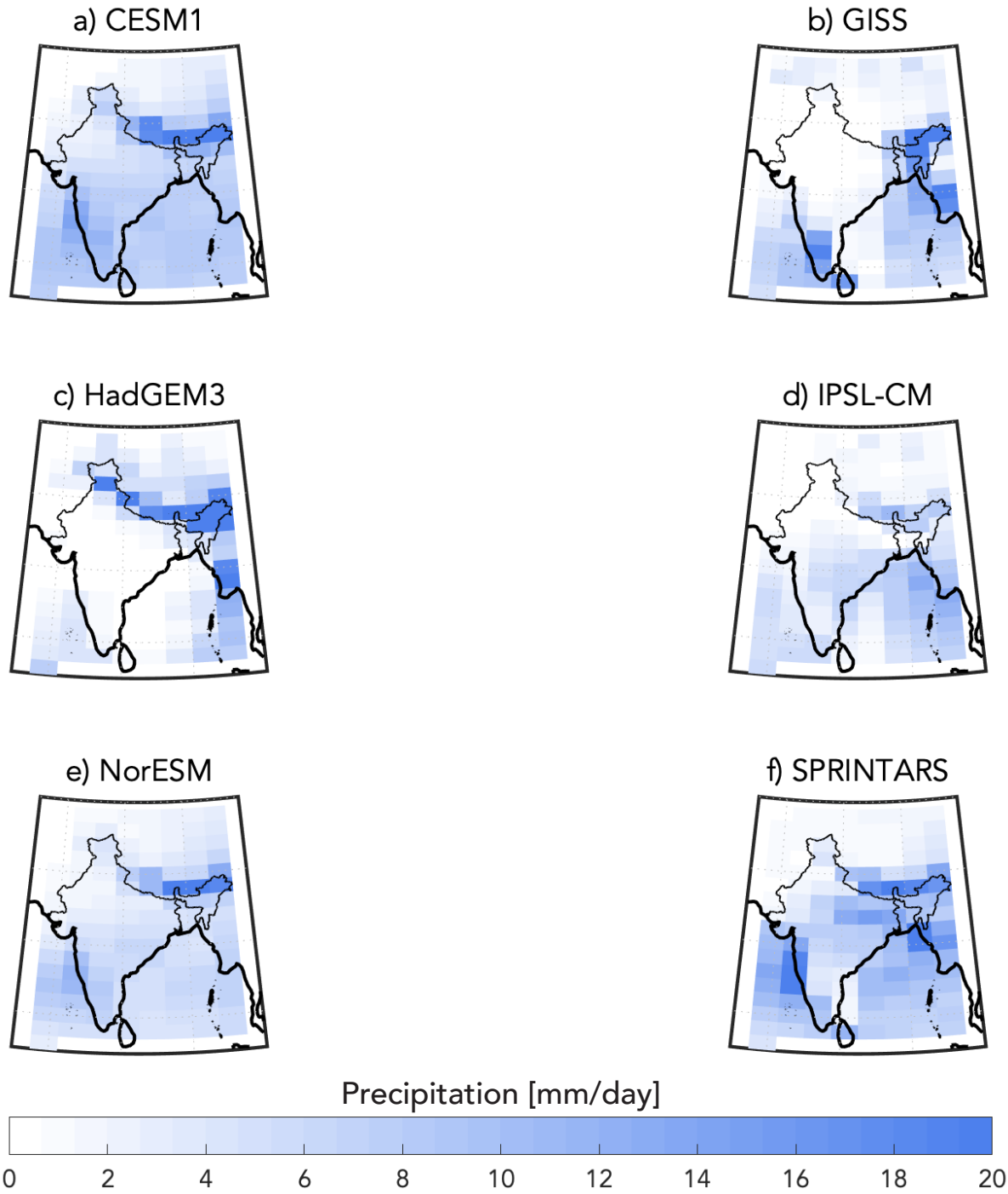

Figure S3. JJAS precipitation mean [mm/day] for the control PDRMIP simulations.

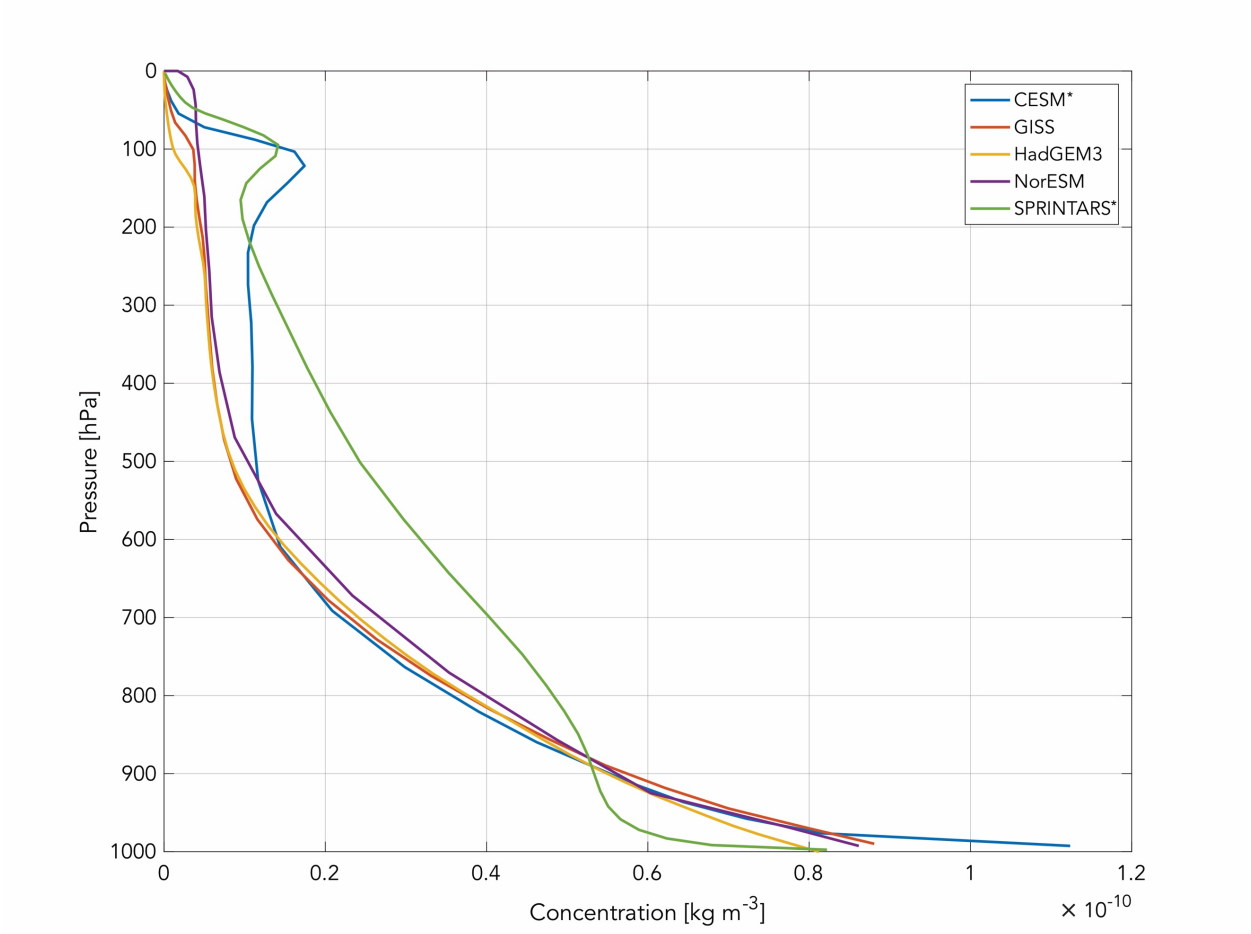

Figure S4. Mean JJAS BC vertical profiles over land in India in the BC10xASIA PDRMIP experiments. Each line indicates a different model within the PDRMIP ensemble. Asterisks denote models that change emissions in the PDRMIP experiments.

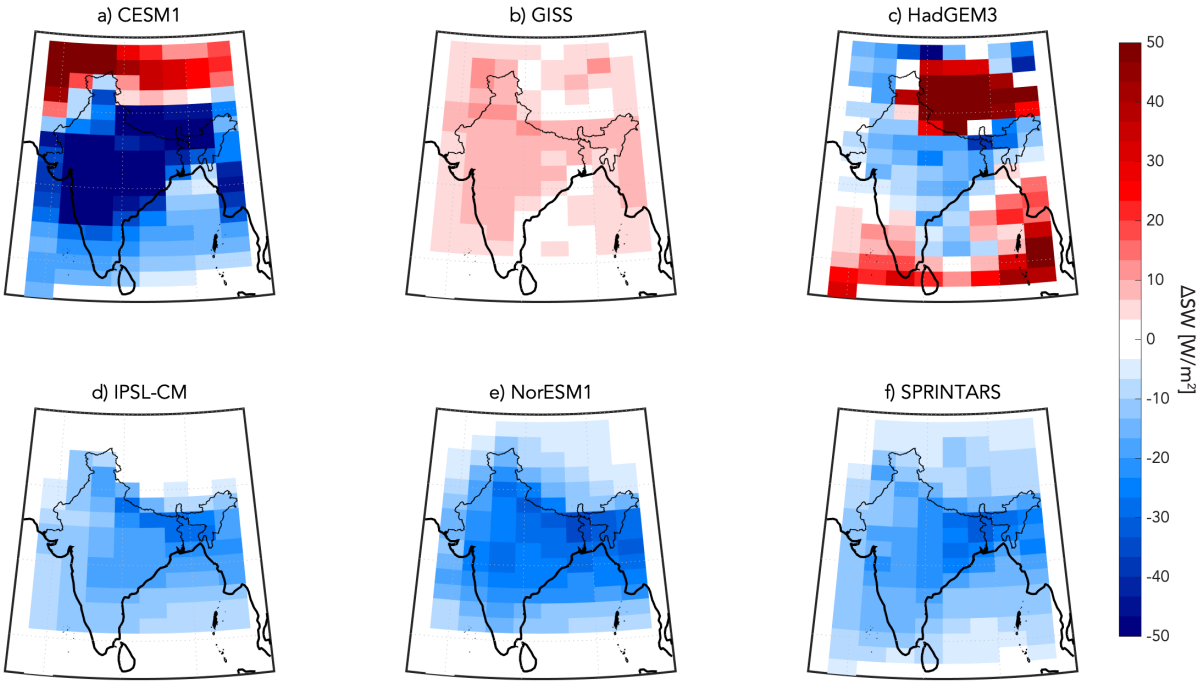

Figure S5. PDRMIP JJAS difference in downward surface shortwave radiation [W/m^2] between BC10xASIA and CTRL$_{PDRMIP}$.

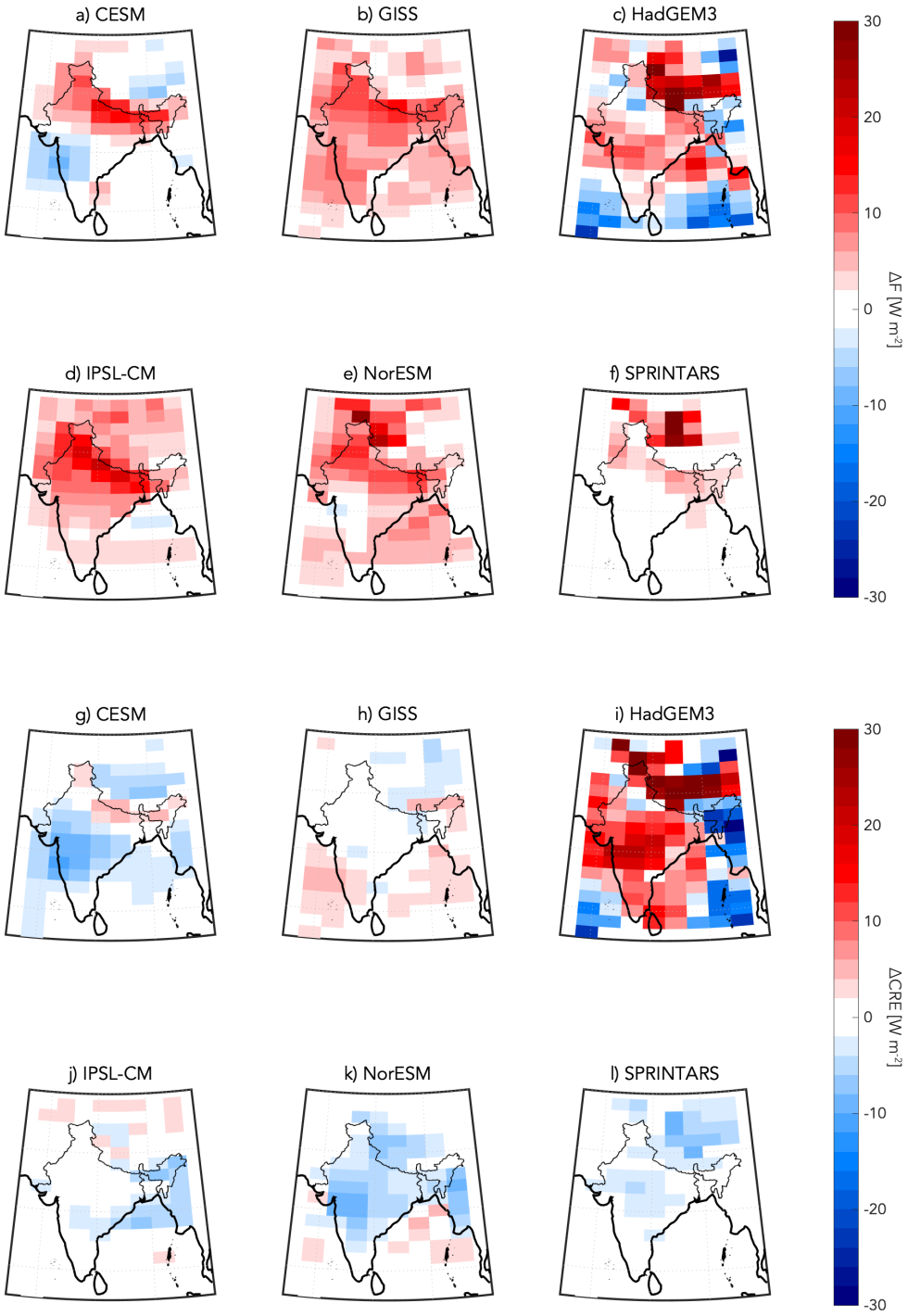

Figure S6. PDRMIP JJAS difference in (a-f) TOA net downward flux [Wm^{-2}] between BC10xASIA and $CTRL_{PDRMIP}$. (g-l) are identical plots for cloud radiative effect.

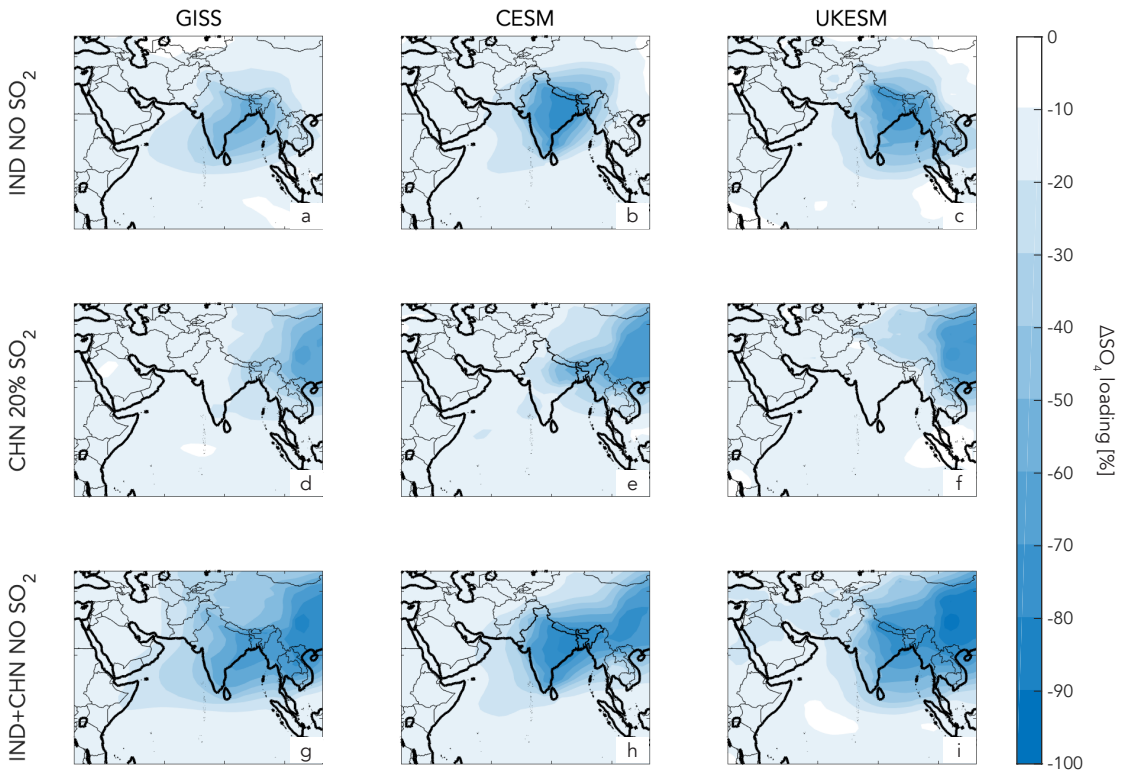

Figure S7. Percentage difference in SO_4 burden between the RAEI SO_2 emissions scenarios and the CTRL runs. The columns represent the different models and rows represent the different emissions scenarios.

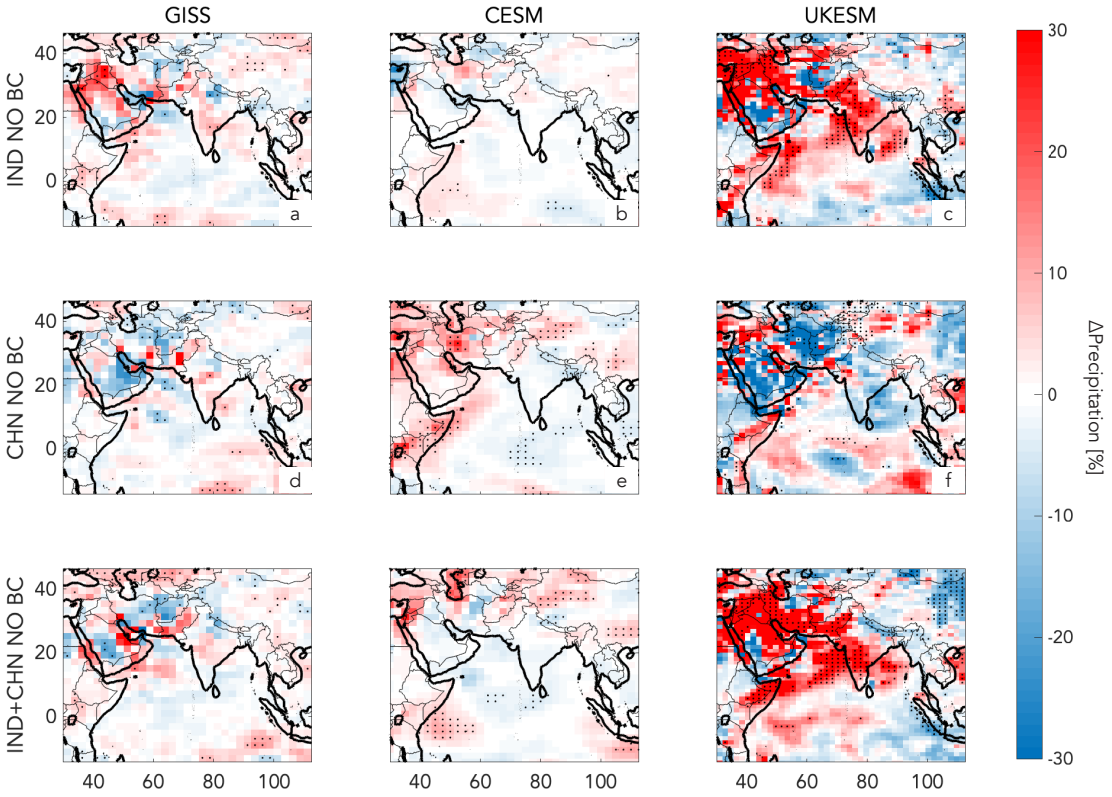

Figure S8. JJAS precipitation percentage difference between the BC regional emissions scenarios and the CTRL runs. The columns represent the different models and rows represent the different emissions scenarios. Stippled regions denote areas where the difference is significant at a 90% confidence level for a two-sample t-test.

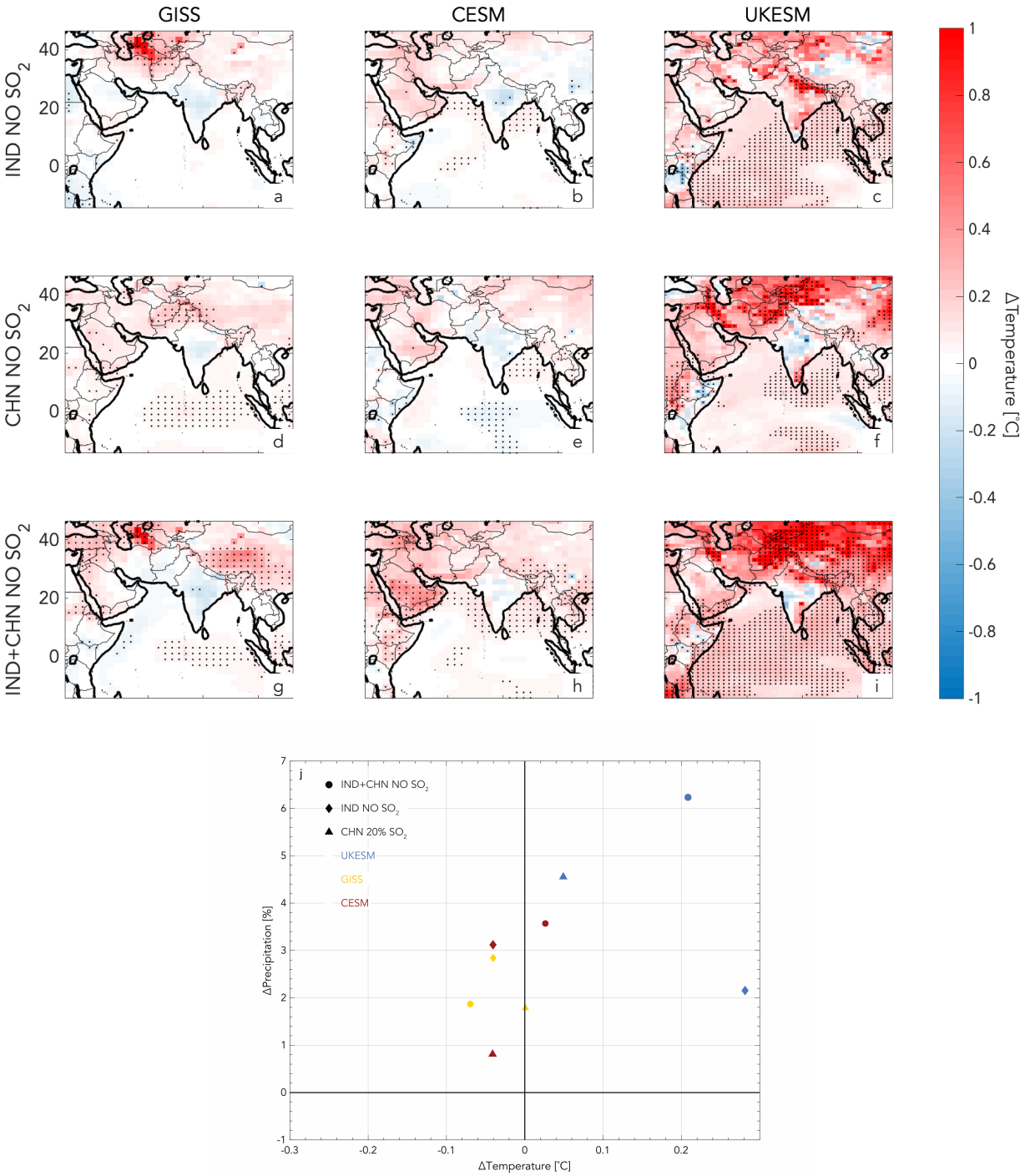

Figure S9. (a-i) Surface temperature difference [˚C] between the RAEI SO_2 emissions scenarios and the CTRL runs. The columns represent the different models and rows represent the different emissions scenarios. Stippled regions denote areas where the difference is significant at a 90% confidence level for a two-sample t-test. (j) Contributions from the SO_2 emissions scenarios on JJAS land temperature and land precipitation. Contributions are represented by the difference between the SO_2 regional emissions scenarios and the CTRL runs over India. Different shapes indicate the different scenarios and different colors indicate the different models as noted in the legend.

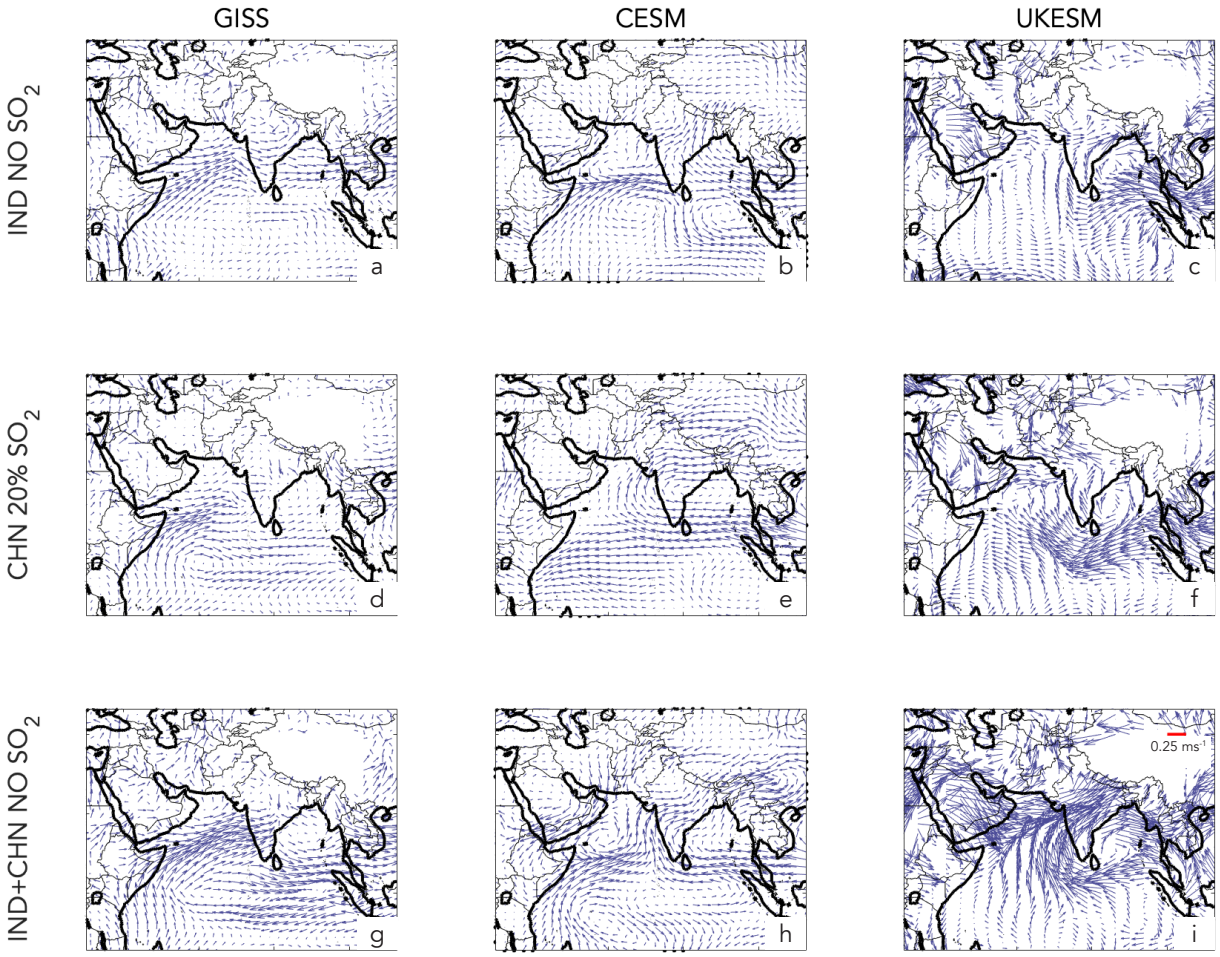

Figure 10. JJAS 850 hPa wind changes between the SO_2 regional emissions scenarios and the CTRL runs. The columns represent the different models and rows represent the different emissions scenarios. A reference arrow indicating 0.25 ms^{-1} is indicated in red in panel i.

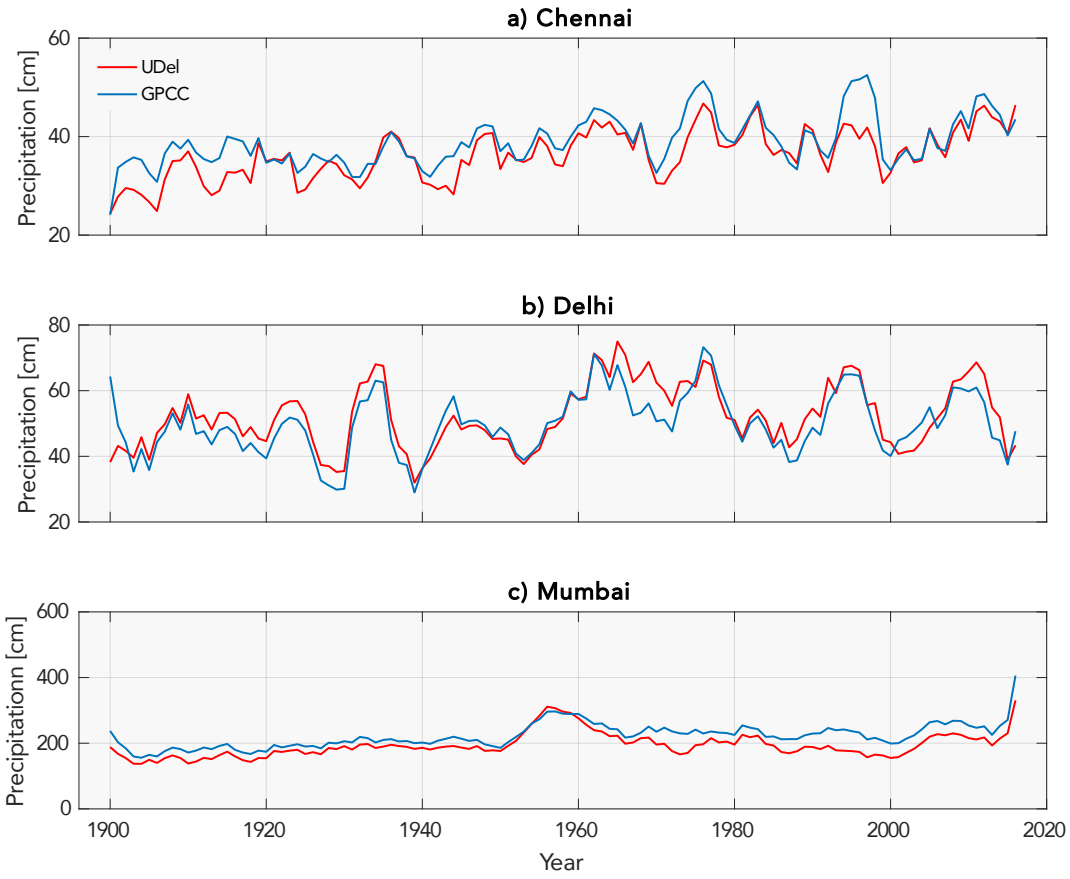

Figure S11. Cumulative summer (JJAS) precipitation [cm] over India from 1900 to 2016 for two observational datasets: (red) University of Delaware (UDel; Willmot and Matsuura, 2001) (blue) the Global Precipitation Climatology Center (GPCC; Schneider et al. 2018). Data are smoothed using a moving mean with a window size of five years. Each panel indicates historical precipitation at a populous city in different regions of India: a) Chennai (southeast), b) Delhi (northeast) and c) Mumbai (northwest).

References

Hoesly, R. M., et al., 2018: Historical (1750–2014) anthropogenic emissions of reactive gases and aerosols from the Community Emissions Data System (CEDS), *Geosci. Model Dev.*, **11**, 369-408.